Supplement of Atmos. Chem. Phys., 26, 3637–3652, 2026
https://doi.org/10.5194/acp-26-3637-2026-supplement

Supplement of

Parametrizing the mixing by clear air turbulence in the chemistry climate model EMAC and its respective radiative impact

Chun Hang Chau et al.

Correspondence to: Chun Hang Chau (cchau@uni-mainz.de)

```
&CTRL

! cat_param describes the approach how to calculate turbulence
!            1 = Ellrod + Knox (DVSI + DVT)
cat_param = 1

! nhours describes the length of the interval for which the divergence
                                     trend term should be calculated, e.g. 6 hours
nhours = 6.

! DIV_C is a weighting constant to limit the amplitude of the divergence trend term
DIV_C  = 0.025

! N2_lim is the limitation threshold for modifying the stability term, mixing will
                         be switched off at the grid box that N2 is  below N2_lim
N2_lim = 6.e-4

! t_norm1 & t_norm2 is the time normalization factor to moderate the strength
                                                           of the whole mixing term
t_norm_1 = 86400
t_norm_2 = 1.344.e6

! logical switch for performing tracer mixing by CAT
l_tracmix = .TRUE.

!use original Ellrod + Knox index for mixing, else use an index modified with N2
USE_DDVSI = .FALSE.
```

Figure S1. Example Fortran90 namelist for the new submodel CAT.

An example of the Fortran90 namelist of the CAT submodel is shown in Figure S1. The namelist including 8 parameters:

- cat_param
- nhours
- DIV_C
- N2_lim
- t_norm1
- t_norm2
- l_tracmix
- USE_DDVSI

The cat_param determines the approach of how to calculate turbulence, currently the Ellrod-Knox index is the only option, but it provides the possibility to extend the submodel to other turbulence diagnostics. The nhours represents the length of the interval (h2 and h1 in equation 1) for which the divergence trend term should be calculated. DIV_C is the constant C in equation 1 and $N2\_lim$ is the N^2_{lim} in equation 2. t_norm_1 and t_norm_2 are used to calculate the t_norm in equation 4, where the former is the seconds of a day and later is the time scaling factor. $l\_tracmix$ is a logical switch for enabling the tracer mixing by CAT. It could be switched to false as a diagnostic submodel for calculating the turbulence diagnostics. The USE_DDVSI could switch between the Ellrod-Knox index and the MoCATI.

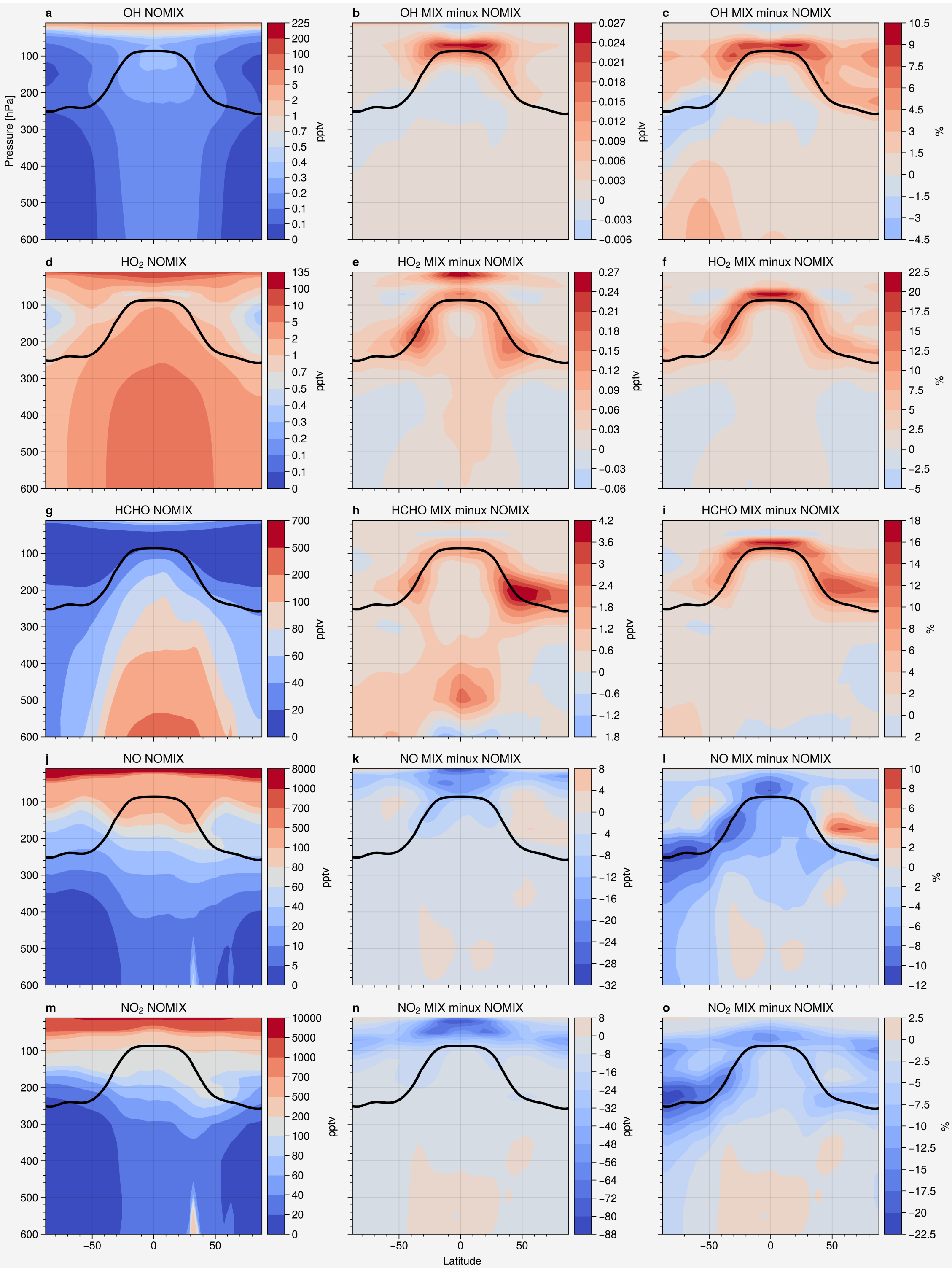

Figure S2. Annual zonal mean OH, HO_2, HCHO,NO, NO_2 (a,d,g,j,m) profile of QCTM-NOMIX, (b,e,h,k,n) difference, (c,f,i,l,o) percentage difference. The black line indicates the tropopause.

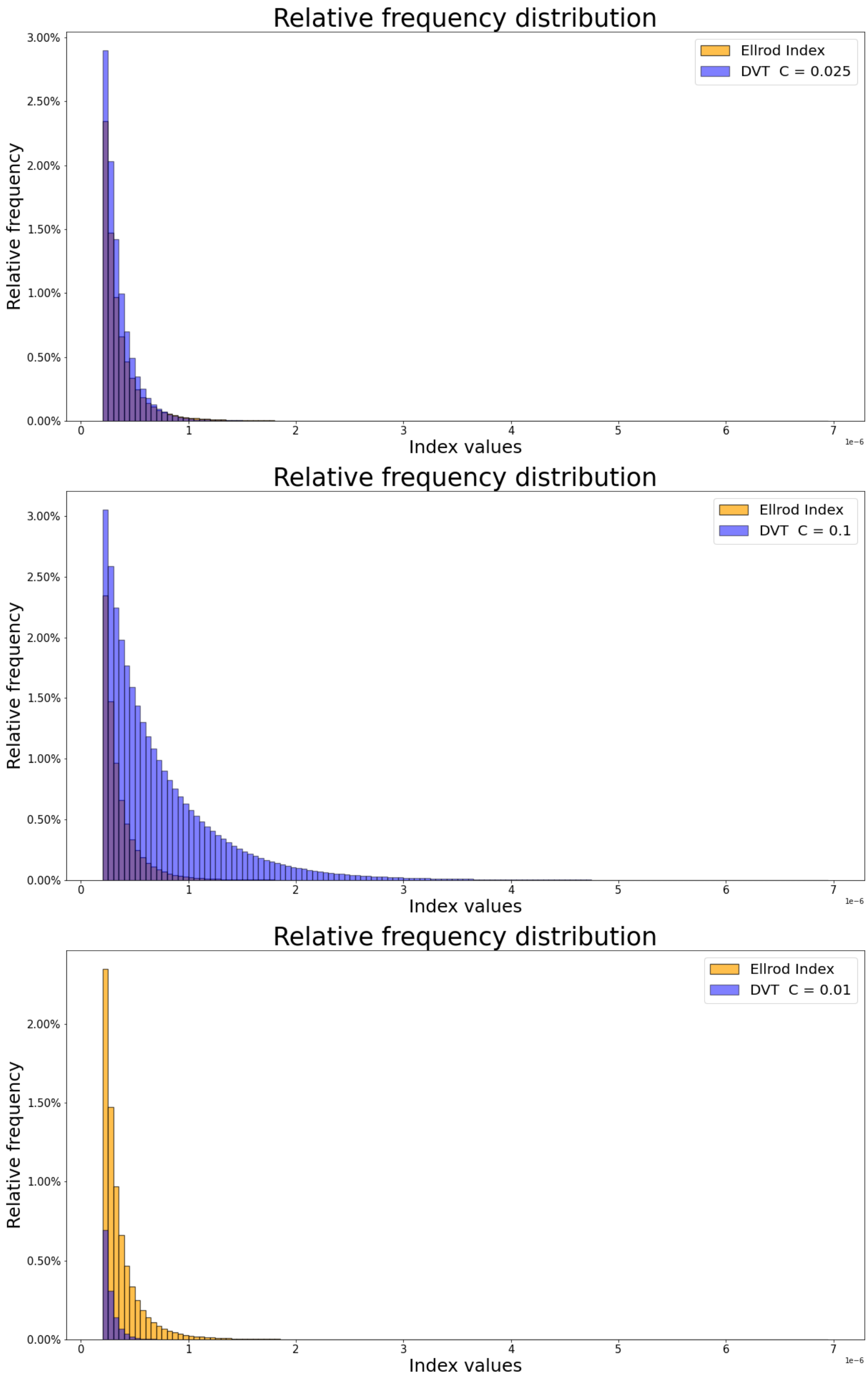

Figure S3. Frequency distribution of different C for DVT (DIV_C) with Ellrod Index. C = 0.025 (top), C = 0.1 (middle), C = 0.01 (bottom).

S1 Evaluation of the newly introduced MoCATI

In order to examine the validity of the MoCATI, we performed statistical tests and calculated the relative frequency distribution of the turbulence diagnostics following the approch of Kaluza et al. (2022), using the ERA5 data for three boreal winters (DJF) from December 2016 to February 2019 over the North Atlantic to calculate and compare the distribution between the well-established Ellrod-Knox index and the MoCATI, but instead of just covering the flight tracks as in Kaluza et al. (2022), we perform calculations on the whole North Atlantic. The constant C for DVT used in this analysis is 0.01 and N^2_{lim} is 6e-4. The North Atlantic winter is found to have the most vertical wind shear (Kaluza et al., 2021). Figure S4 shows a map of the domain from 60° W to 0° W and 35° N to 60° N for the Ellrod-Knox index and MoCATI at the lapse rate tropopause (temperature lapse rate decreases to 2 K/km or less and stays on average below this value between this altitude level and any level above with the next 2 km) on 01 December 2016. Both indices show a similar distribution, although the magnitude of MoCATI is weaker considering it is constrained by the additional stability term. Figure S5 shows the Taylor diagram using the Ellrod-Knox index as a reference. It shows the correlation coefficient, normalized standard deviation and the normalized root-mean squared difference (both normalized with the reference standard deviation from the Ellrod-Knox index). As expected, the MoCATI shows a similar behaviour on these statistical metrics since it is a modification of the Ellrod-Knox index. The MoCATI is highly correlated, with a similar normalized standard deviation close to the perfect 1.0 line, and a small RMSD of half of the reference standard deviation. Figure S5 also includes the Ellrod index (TI), vertical wind shear (VWS) and deformation (DEF). Although the TI, VWS and DEF are included as part of the Ellrod-Knox index, since an additional divergence trend term is added, they show a lower correlation with the Ellrod-Knox index compared to the MoCATI. Figure S6 shows the relative frequency distribution of the ln(MoCATI) and ln(Ellrod-knox index) by geometric height and distance relative to the lapse rate tropopause. Both indices show a similar distribution, with a rightward shift (i.e., stronger turbulence) at lower altitudes and a leftward shift at higher altitudes. MoCATI has a more prominent leftward shift at higher altitudes considering the additional static stability term which constrains the index. We also perform a ROC (Receiver operating characteristic) analysis to examine the performance of the Ellrod-Knox index and MoCATI using TI as the classification threshold (Sharman et al., 2006). Both indices show a similar performance under different thresholds (Figure S7). To conclude, the newly introduced MoCATI shows a comparable performance with the well-established Ellrod-Knox index, but takes the static stability into account, modifying the effective mixing of tracer under specific temperature profile conditions.

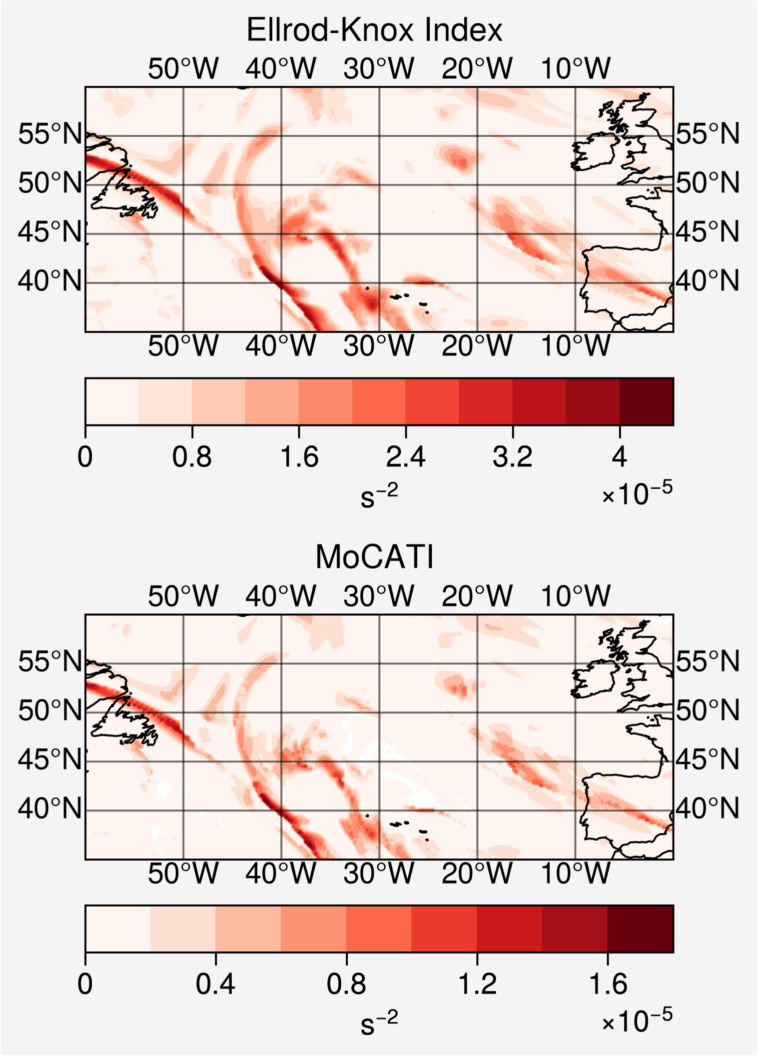

Figure S4. Map of the Ellrod-Knox index and MoCaTI at the lapse rate tropopause on 01 Dec 2016 1600 UTC.

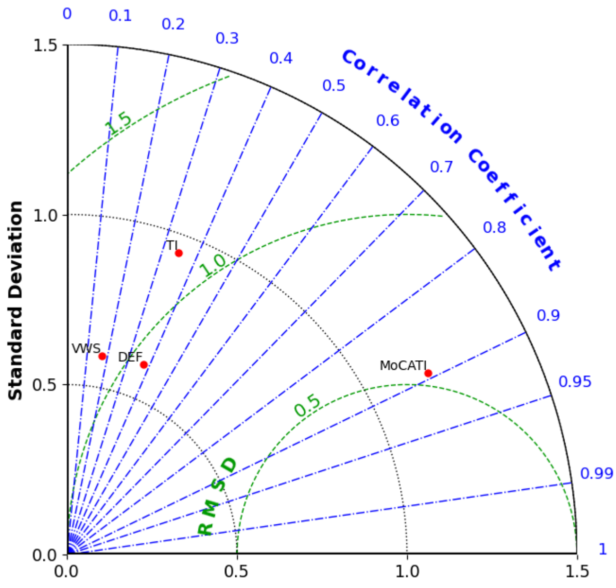

Figure S5. Taylor diagram showing the correlation coefficient, normalized standard deviation and normalized root mean square difference (RMSD) using the Ellrod-Knox index as reference.

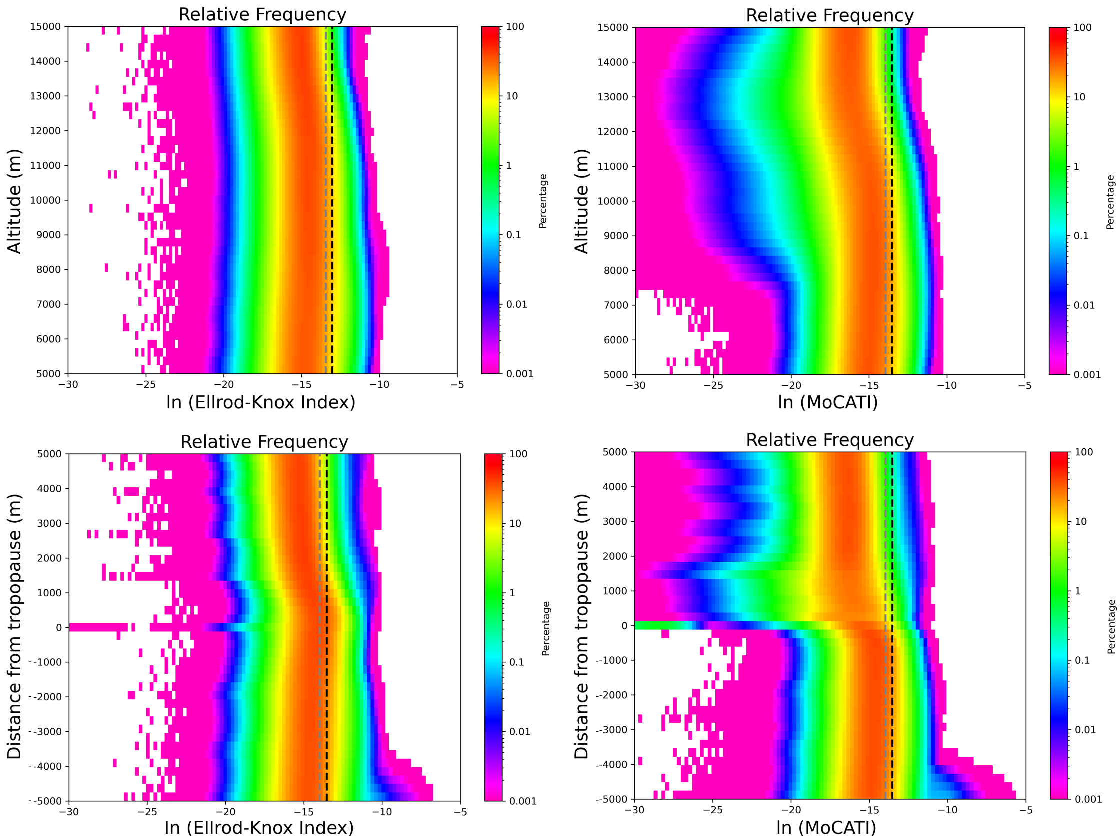

Figure S6. Relative frequency distribution for MoCATI (left) and Ellrod-Knox index (right) in geometric height (top) and relative to the lapse rate tropopause (bottom). Dashed lines indicate the 95th percentile (black) and 90th percentile (grey).

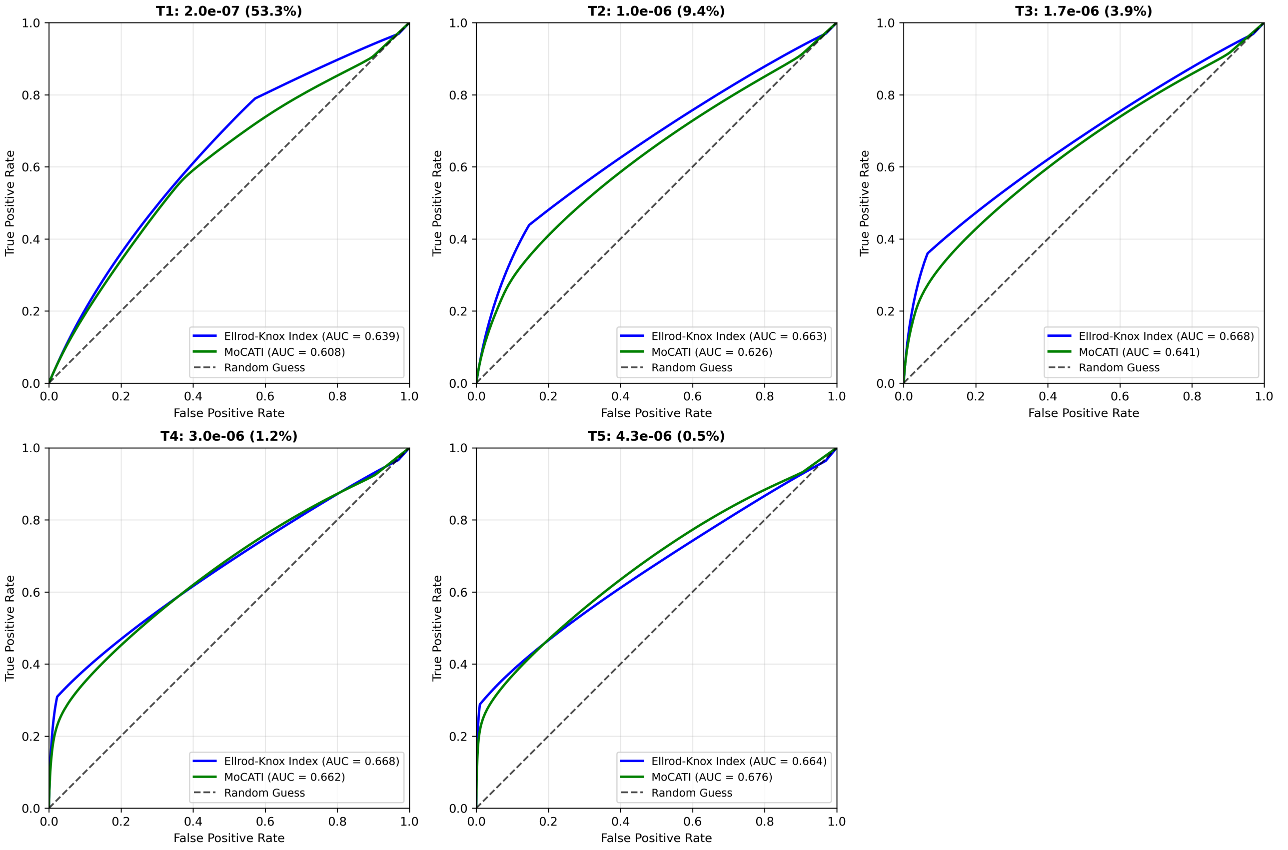

Figure S7. ROC curves showing the probability of false detection and true detection for Ellrod-Knox index and MoCATI using different TI as threshold: T1 = null, T2 = light, T3 = moderate, T4 = severe and T5 = extreme. The brackets represent the percentage of data that reaches the corresponding threshold. AUC represents the area under the curve.

References

Kaluza, T., Kunkel, D., and Hoor, P.: On the occurrence of strong vertical wind shear in the tropopause region: a 10-year ERA5 northern hemispheric study, Weather and Climate Dynamics, 2, 631–651, https://doi.org/10.5194/wcd-2-631-2021, 2021.

Kaluza, T., Kunkel, D., and Hoor, P.: Analysis of Turbulence Reports and ERA5 Turbulence Diagnostics in a Tropopause-Based Vertical Framework, Geophysical Research Letters, 49, e2022GL100 036, https://doi.org/https://doi.org/10.1029/2022GL100036, e2022GL100036 2022GL100036, 2022.

Sharman, R., Tebaldi, C., Wiener, G., and Wolff, J.: An Integrated Approach to Mid- and Upper-Level Turbulence Forecasting, Weather and Forecasting, 21, 268 – 287, https://doi.org/10.1175/WAF924.1, 2006.